Title

Quantification of hemodynamics of cerebral arteriovenous malformations after stereotactic radiosurgery using 4D flow magnetic resonance imaging

Journal

Journal of Magnetic Resonance Imaging, 53(6)

ISSN

1053-1807

Authors

Srinivas, Shanmukha
Retson, Tara
Simon, Aaron
et al.

Publication Date

2021-06-01

DOI

10.1002/jmri.27490

Peer reviewed

HHS Public Access

Author manuscript

J Magn Reson Imaging. Author manuscript; available in PMC 2022 June 01.

Published in final edited form as:

J Magn Reson Imaging. 2021 June ; 53(6): 1841–1850. doi:10.1002/jmri.27490.

Quantification of hemodynamics of cerebral arteriovenous malformations after stereotactic radiosurgery using 4D Flow MRI

Shanmukha Srinivas[1], **Tara Retson**[1], **Aaron Simon**[2], **Jona Hattangadi-Gluth**[2], **Albert Hsiao**[1], **Nikdokht Farid**[1]

[1]Department of Radiology, University of California-San Diego, San Diego, California, USA.

[2]Department of Radiation Medicine and Applied Sciences, University of California-San Diego, San Diego, California, USA.

Abstract

Background: Stereotactic radiosurgery (SRS) is used to treat cerebral arteriovenous malformations (AVM). However, early evaluation of efficacy is difficult as structural MRI/MRA often does not demonstrate appreciable changes within the first 6 months.

Purpose: To evaluate the use of 4D flow MRI to quantify hemodynamic changes after SRS as early as 2 months.

Study Type: Retrospective observational

Subjects: 14 patients with both pre-SRS and post-SRS imaging obtained at multiple timepoints from 1–27 months after SRS

Field Strength/Sequence, Assessment: 3T; T_2 Single Shot Fast Spin Echo, time-of-flight (TOF) magnetic resonance angiography (MRA), and postcontrast 4D flow with 3D velocity encoding between 150 and 200 cm/s

Assessment: Post-hoc 2D cross sectional flow was measured for the dominant feeding artery, the draining vein, and the corresponding contralateral artery as a control. Measurements were performed by two independent observers, and reproducibility was assessed.

Statistical Tests: Wilcoxon signed-rank tests were used to compare differences in flow, circumference, and pulsatility between the feeding artery and the contralateral artery both before and after SRS; and differences in nidus size and flow and circumference of the feeding artery and draining vein before and after SRS.

Results: Arterial flow (L/min) decreased in the primary feeding artery (mean: 0.1 ± 0.07 vs 0.3 ± 0.2; $p < 0.05$) and normalized in comparison to the contralateral artery (mean: 0.1 ± 0.07 vs 0.1 ± 0.07; $p = 0.068$). Flow decreased in the draining vein (mean: 0.1 ± 0.2 vs 0.2 ± 0.2; $p < 0.05$), and the circumference of the draining vein also decreased(mean: 16.1 ± 8.3 vs 15.7 ± 6.7; $p < 0.05$). AVM volume decreased after SRS (mean: 45.3 ± 84.8 vs 38.1 ± 78.7; $p < 0.05$). However,

Corresponding Author: Nikdokht Farid MD, Professor of Radiology, University of California – San Diego, 200 West Arbor Drive, San Diego, CA 92103, Phone: (858) 837 - 0744, nfarid@health.ucsd.edu.

circumference (mm) of the primary feeding artery remained similar after SRS (mean: 15.7 ± 2.7 vs 16.1 ± 3.1; p=0.600).

Conclusions: 4D flow may be able to demonstrate early hemodynamic changes in AVMs treated with radiosurgery, and these changes appear to be more pronounced and occur earlier than the structural changes on standard MRI/MRA.

Keywords

Cerebral Arteriovenous Malformations; Stereotactic Radiosurgery; 4D flow MRI; Hemodynamics

Introduction

In arteriovenous malformations (AVMs), the normal capillary bed is disrupted by aberrant angiogenesis[1]. The incidence of brain AVMs is approximately 18 per 100,000 people[2]. Every year about 4 percent of individuals with untreated cerebral AVMs will experience hemorrhage, which often leads to severe morbidity or death[3].

For small AVMs with high risk of complications from surgical resection, stereotactic radiosurgery (SRS) is a standard treatment[4]. SRS causes fibro-intimal damage of the endothelium of the arteries supplying the AVM, eventually leading to nidus obliteration[5]. There may be risk of rupture and hemorrhage during the latency period between SRS and nidus obliteration. Therefore, the ability to monitor early treatment response following SRS is critical for guiding appropriate clinical management.

After SRS, the most common strategy to monitor AVMs includes post-treatment MRI repeated at regular intervals, usually at a minimum of 6 months post-treatment, to follow AVM resolution. Once complete resolution is visualized, angiography is performed to confirm obliteration of the AVM nidus[6–10]. Obliteration of AVM on digital subtraction angiography (DSA) is defined as absence of AV shunting or disappearance of AVM nidus and early draining veins[9, 11–13]. DSA is the most sensitive imaging modality to follow AVMs, but it is not routinely performed as it is invasive and carries various risks including stroke[14]. Moreover, structural changes on DSA and MRI may take several years to occur[15]. Hemodynamic parameters including arterial flow, wall shear stress, and venous hypertension have been proposed as key predictors of cerebral AVM hemorrhage[16].

The advent of 4D flow MRI, a time-resolved, phase-contrast imaging technique, has led to assessment of cerebral blood flow with improved spatial and temporal resolution[17]. Quantitative measurements of blood flow with 4D flow MRI have been found to be highly reproducible to guide management of patients with congenital and acquired structural heart disease[18, 19]. Studies have suggested cerebral 4D flow MRI measurements correlate well with 2D phase-contrast MRI (PC-MRI) and transcranial doppler ultrasound[20]. Despite limited resolution in smaller arteries such as the ophthalmic artery and communicating arteries, 4D flow MRI has been shown to be reliable in measuring the flow in the major arteries of the circle of Willis in healthy patients[21, 22]. Given the limitation in measuring treatment response with existing structural imaging techniques, this study investigated the

use of 4D flow to elucidate the hemodynamic characteristics of AVMs before and after treatment with SRS.

Materials and Methods

Institutional Review Board Approval

This retrospective study was approved by the Institutional Review Board with waiver of informed consent. The study was a retrospective analysis of an observational imaging dataset, that was prospectively and longitudinally maintained for cerebral AVM patients who were treated and imaged at one institution.

Clinical Follow-Up

A total of 14 patients, 6 females and 8 males, were included in this study. All patients included in this study were treated, managed and followed by a CNS radiation oncologist with 8 years of neurovascular expertise (JHG). Patients who proceeded with SRS received follow-up imaging as deemed clinically appropriate. Patients who had imaging inclusive of 4D flow MRI before and after SRS were included. Patients who received SRS prior to the study who did not receive a baseline examination with 4D flow MRI were excluded from analysis. Figure 1 shows the patients included in this study and time points of respective 4D flow measurements. Of note, not all patients underwent imaging at the same frequency or interval, as this was a retrospective review of patients undergoing MRI for clinical management.

Data Collection

As part of a standard protocol, patients underwent 4D flow MRI, 3D Time-of-flight (TOF) MRA, and T_2-weighted single shot fast spin echo (SSFSE) MRI on a 3T GE Discovery 750 MRI scanner (GE Healthcare, Milwaukee, Wisconsin) using a 16-channel head/neck/spine coil. This included administration of gadobenic acid 0.1 mmol/kg contrast. T_2-weighted SSFSE MRI was acquired with the following parameters – slice thickness 4 mm, average echo time (TE) 88.6 seconds (81.44–114.00 seconds), average repetition time (TR) 6299.59 seconds (2895.00–8660.00 seconds), average flip angle 105.5 ^{o} (90–111^{o}), and acquisition time 3 – 4 minutes.

TOF MRA was acquired with the following parameters – slice thickness 1 mm, average echo time (TE) 2.6 seconds (2.3–5.7 seconds), average repetition time (TR) 24.3 seconds (22.00–30.00 seconds), flip angle 15 ^{o} and acquisition time 5 – 6 minutes.

4D flow data was acquired using a parallel-imaging compressed-sensing variant with variable-density Poisson sampling and ESPIRiT reconstruction with the following parameters – acquired resolution 1.10 × 0.96 × 1.70 mm (1.07–1.12 × 0.94–0.98 × 1.60–1.20 mm), reconstructed resolution 0.96 × 0.96 × 0.88 mm (0.94–0.98, 0.94–0.98, 0.8–1.6 mm), average scan time 8 minutes 28 seconds (4 minutes 57 seconds – 13 minutes 34 seconds), velocity encoding (VENC) 150–200 cm/s, bandwidth 62 KHz, flip angle 15^{o}, average repetition time (TR) 5.01 seconds (4.83–5.29 seconds), average echo time (TE) 2.44

seconds (2.38–2.52 seconds), and total acceleration factor of 1.8 (1.6 – 2.0) in the phase direction and 2.0 (1.6–2.0) in the slice direction.

Patient charts were reviewed for age at start of treatment, sex, AVM location, Spetzler-Martin grade, treatment, and dose of radiation.

Magnetic Resonance Imaging Processing

Prior to performing measurements, background phase (eddy current) errors were corrected. Eddy current errors were corrected by adjusting blood and anatomy filters, and delineating non-static masks for blood flow in Arterys Cardio AI v2.2 (Arterys, San Francisco, CA) while Maxwell terms and gradient field non-linearity were corrected automatically inline with image reconstruction[23].

Regions of aliasing were identified on phase image and excluded from blood flow analysis. 4D flow measurements were performed by a graduate level research student, SS, with 2 years of experience in cerebrovascular 4D flow MRI under the supervision of a faculty neuroradiologist with 10 years of brain imaging experience (NF).

AVM nidus volume was measured on T_2-weighted images by NF. AVMs which were larger than 3 cm in length, height, width, and volume ≥ 27 cm^3 were classified as large.

Posthoc 2D cross-sectional flow and circumference were measured for the dominant feeding artery, dominant draining vein and corresponding contralateral artery. Pulsatility index was calculated for each arterial measurement as:

$$pulsatility\ index = (peak\ systolic\ flow - minimum\ diastolic\ flow)/(peak\ systolic\ flow). \quad (1)$$

Single measurement locations were proximal to the AVM and for each patient, the same measurement locations were used at each consecutive time point. For AVMs with multiple feeding arteries and draining veins, the feeding artery and draining vein with the highest blood flow, as determined by 2D cross sectional analysis, were designated as the dominant artery and dominant vein.

To assess interobserver reproducibility for flow measurements, TR, a radiology resident with 4 years of experience in cerebrovascular imaging, also measured ipsilateral, contralateral, and venous flow. To assess interobserver reproducibility for volume measurements, SS, a graduate student with 2 years of experience in cerebrovascular imaging, also measured AVM nidus volume on T_2-weighted MRI.

Statistical Analysis

Statistical analysis was performed using RStudio Version 1.3.1056. For patients with multiple time points of imaging after SRS, the most recent MRI up to 16 months post-SRS was included for statistical analysis with a median time interval of 12 months (range: 11–16 months) following SRS. With a limited sample size and non-normal distribution, the assumptions for performing a parametric test were not met, so a Wilcoxon signed-

rank test was performed to evaluate differences in flow, circumference, and pulsatility between the ipsilateral and contralateral artery both before and after SRS. Differences in flow, circumference, and pulsatility of the ipsilateral artery before and after SRS were also assessed using a Wilcoxon signed-rank test. Following this, differences in flow and circumference of the draining vein before and after SRS were assessed using a Wilcoxon signed-rank test.

Differences in AVM nidus volume before and after SRS were also assessed using a Wilcoxon signed-rank test. A secondary analysis assessed differences in flow and volume between small (volume < 27 cm^3) and large (volume ≥ 27 cm^3) AVMs using a Wilcoxon signed-rank test. P values less than 0.05 were considered significant.

Intraclass coefficient (ICC) was computed for interobserver reproducibility of pre-SRS and post-SRS flow and volume measurements as part of a two-way mixed effects model. ICC was categorized as poor (< 0.5), moderate (0.5 – 0.75), good (0.76 – 0.9), or excellent (> 0.9) for flow and volume measurements.

Results

Patient Characteristics

The average age at start of treatment was 44.3 years (range: 21 – 76). The Spetzler-Martin (SM) Grades were as follows: SM 2 (3), SM 3 (7), SM 4 (2), SM 5 (2). The median Spetzler-Martin grade was 3. Five patients underwent embolization, two patients underwent coiling, and one patient underwent surgical resection of their AVM prior to SRS. Eleven patients received single-stage SRS while three patients received multiple stages of SRS. The average dose of radiation delivered was 1996 cGy in a single fraction (range: 1600–2200 cGy). Table I lists these patient characteristics.

Illustrative Cases

Figures 2 and 3 illustrate structural and hemodynamic changes for two patients, one with a small volume AVM and one with a large volume AVM, respectively.

Aggregate Flow, Pulsatility, Vessel Circumference, and AVM Volume

Figure 4 illustrates the aggregate arterial and venous flow, vessel circumference, and pulsatility, as well as AVM volume for all patients in this cohort. Of note, three patients received multiple stages of SRS and had 4D flow measurements in between treatments. There is a rapid early decrease in flow within the feeding artery, in contrast to a more gradual decrease in AVM volume.

Average Changes in Ipsilateral and Contralateral Artery (Figure 5)

Arterial flow (L/min) decreased in the AVM primary feeding artery post-SRS (0.1 ± 0.07) compared to pre-SRS (0.3 ± 0.2) ($p < 0.05$, df = 13). Pre-SRS, arterial flow (L/min) was higher in the AVM primary feeding artery than in the contralateral arterial control (contralateral: 0.1 ± 0.05) ($p < 0.05$, df = 13). Post-SRS, the flow differential (L/min)

between the feeding artery (0.1 ± 0.07 L/min) and the contralateral artery (0.1 ± 0.07) was not statistically different (p = 0.068, df = 13).

Pre-SRS, arterial circumference (mm) was higher in the primary feeding artery (16.1 ±3.1) than in the contralateral arterial control (13.5 ±2.1) (p < 0.05, df = 13). Post-SRS, the circumference of the feeding artery did not significantly decrease (15.7±2.7) (p=0.358, df = 13). The circumference differential between the feeding artery (15.7±3.2) and the contralateral artery (13.4±2.2) remained significant post-SRS despite the changes in flow (p < 0.05 , df = 13). Pre-SRS, pulsatility index was significantly lower in the primary feeding artery (0.4 ±0.1) than in the contralateral arterial control (0.7±0.1) (p < 0.05, df = 13). Post-SRS, pulsatility index increased significantly in the AVM primary feeding artery (0.6±0.2) in comparison to pre-SRS (0.4±0.1) (p < 0.05, df=13). Post-SRS, the pulsatility differential between the feeding artery (0.6±0.2) and the control artery (0.5±0.2) was less pronounced and not statistically different (p = 0.761, df=13).

Average Changes in Venous Flow and Circumference (Figure 6)

Flow (L/min) decreased significantly in the draining vein post-SRS (0.1± 0.2) compared to pre-SRS (0.2±0.2) (p < 0.05, df = 13) and circumference of the draining vein also decreased post-SRS (15.7±6.7) compared to pre-SRS (16.1±8.3) (p < 0.05, df = 13).

Volume Analysis (Figure 5)

AVM Nidus volume decreased significantly post-SRS (38.1±78.7) compared to pre-SRS (45.3±84.8) (p < 0.05 , df = 13). However, in a subset analysis of small and large AVMs, volume (cm^3) did not decrease significantly for large AVMs (pre-SRS: 138.1 ± 121.8 vs. post-SRS: 125.4 ± 111.9) (p = 0.181, df = 3), but there was a significant reduction in volume (cm^3) for small AVMs (pre-SRS: 6.7 ± 10.7 vs. post-SRS: 3.2 ±5.9) (p < 0.05, df = 9).

Interobserver Variability

The ICC for AVM nidus volume measurements was 0.998 (95% CI: 0.996 – 0.999), indicating an excellent agreement between both observers. The ICC for ipsilateral artery flow (0.999, 95% CI: 0.998 – 0.999), contralateral artery flow (0.997, 95% CI: 0.993 – 0.999), and vein flow (1, 95% CI: 1 – 1) also demonstrated excellent agreement between both observers.

Discussion

Existing imaging techniques do not adequately capture treatment response and changes in blood flow within AVMs during the latency period between treatment and nidus obliteration, a critical period of time during which patients are at risk for cerebral hemorrhage. This study demonstrated the use of 4D flow MRI for evaluation of early and sustained hemodynamic changes in patients with cerebral AVMs treated with SRS. In this cohort, hemodynamic changes were observed as early as 2 months post-SRS. These results extend prior findings from a case study demonstrating early hemodynamic response in an AVM following SRS using 4D flow MRI in a single subject[24]. These hemodynamic changes including decreased flow within the feeding artery and draining vein precede structural changes in

arterial circumference.Venous circumference, unlike arterial circumference, was a structural biomarker which did decrease at early timepoints. Of note, although nidus volume decreased for the entire cohort, for patients with large AVMs (≥ 27 cm^3), structural changes in nidus volume are subtle and gradual with minimal changes even at 16 months post-SRS. Therefore, for large AVMs, hemodynamic changes on 4D flow MRI may be even more instrumental in evaluation of treatment response. Moreover, while measuring AVM volume accurately often requires time-intensive techniques such as planimetry due to irregular and varying contours, neurovascular 4D flow MRI has demonstrated high reproducibility[25, 26]. Although SM grade allows peri-operative risk-stratification of AVMs by size, eloquence of adjacent tissue, and presence of deep venous drainage, hemodynamic information could further improve detection of treatment response for cerebral AVMs.

Findings in this study are concordant with prior studies using other imaging techniques to measure blood flow in cerebral AVMs. For example, using transcranial doppler to perform phase shift analysis between cerebral blood flow velocity and arterial blood pressure, it has been shown that resistance is lower in vessels supplying AVMs[27, 28]. Likewise, previous use of 4D flow has demonstrated an abnormal, monophasic waveform with reduced pulsatility in the feeding artery of patients with Spetzler-Martin Grade 4 AVMs[29]. Similarly, this study showed pulsatility was significantly lower in the feeding artery of the AVM than the contralateral artery prior to treatment.

Using quantitative MRA to measure blood flow in cerebral AVMs before and after embolization and surgery, Shakur et al. demonstrated that blood flow in the ipsilateral artery decreased and normalized in comparison to the contralateral artery after both embolization and surgery[30]. This study replicates these findings in this cohort of patients treated with SRS. In contrast, Shakur et al. demonstrated that pulsatility in the ipsilateral artery increased after only surgery and not embolization[30]. They postulated that redistribution of flow after embolization and maintenance of low pulsatility index may be associated with lower rates of rupture. In this study, pulsatility normalized in the feeding artery post-SRS, compared to the contralateral artery, and significantly increased post-SRS compared to pre-SRS. These results may reflect how SRS results in structural changes within the vasculature of AVMs. Structural changes in the arterial wall, such as hyaline sclerosis and endothelial-intimal damage, may decrease elasticity of the vessel and increase the pulsatility index of distal arterial flow just as carotid intimal-medial thickness increases middle cerebral artery pulsatility index in atherosclerosis[31]. Further studies of 4D flow for AVMs treated by embolization or surgery may help better elucidate differences in hemodynamic and structural changes of AVMs after varying treatment modalities.

AVMs can induce global changes in hemodynamics extending beyond the nidus. There is often a change in network level functional and structural plasticity in the setting of aberrant brain anatomy[32, 33]. This can manifest in alteration of connectivity between both hemispheres and could also contribute to alteration in hemodynamics of contralateral brain regions[34]. A previous study in a small cohort of AVM patients demonstrated alterations in hemodynamics of extranidal vessels in comparison to healthy controls using 4D flow[35]. Prior research has also suggested that there is a “steal” phenomenon such that blood flow to the AVM feeding artery is augmented at the expense of the contralateral artery, thereby

leading to contralateral hypoperfusion[36]. This has yet to be proven as a mechanism of focal neurological deficit, however[37]. In this study, contralateral arterial flow did not increase significantly after SRS compared to before SRS. However, the difference between contralateral and ipsilateral flow normalized after SRS. Whether this progression towards symmetric blood flow after SRS was solely due to reduction of flow within the ipsilateral artery or a reversal of steal phenomenon is unknown. In future studies, the presence of steal phenomenon can be further assessed using healthy controls to evaluate changes in contralateral artery flow for patients with AVMs prior to SRS.

Limitations

Cerebral AVMs are relatively rare, and therefore, this study's sample size is limited. Data analysis was performed retrospectively and therefore causal effects of treatment on hemodynamic parameters can be difficult to delineate without controlling for confounding variables. Furthermore, there are limitations associated with the 4D flow technique, including limited resolution in smaller arteries and aliasing in high-flow arteries[21]. To avoid this problem, 2D post-hoc measurements were performed in dominant arteries and veins with a robust caliber and in areas without aliasing. There are several opportunities for further investigation. Follow-up for this study occurred as part of routine clinical management, and therefore there is inherent variability in the scan intervals and frequency. In future studies, it would be ideal to obtain 4D flow measurements at the same interval and with the same frequency for each patient. Structured follow-up guidelines would allow delineation of the natural trajectory of hemodynamic response of AVMs to SRS over time. As 4D flow MRI becomes implemented into clinical practice to monitor hemodynamics of cerebrovascular disorders, integration of machine learning to augment background phase error correction, segment cerebral vessels, and prognosticate patients treated for AVMs will expedite data acquisition and further standardize 4D flow measurements[38, 39].

Conclusion

4D flow MRI demonstrates early hemodynamic changes in cerebral AVMs treated with SRS, including reduction in feeding arterial and draining venous blood flow. These hemodynamic changes may precede structural changes such as circumference of the feeding artery and AVM nidus volume. 4D flow can potentially serve as a powerful adjunct to routine MRI/MRA in monitoring early treatment response of cerebral AVMs following SRS.

Acknowledgments

Grant Support: This work was partially supported by the Radiological Society of North America (RSNA) Resident Research Grants RR1965 (A.S.), RR1879 (T.R); RSNA Medical Student Research Scholarship RMS1825 (S.S.); National Institutes of Health (NIH) grants T32 EB005970 (T.R.), #1KL2TR001444 (JAH-G), R01CA238783–01 (JAH-G). The content is solely the responsibility of the authors and does not necessarily represent the official views of the RSNA or NIH.

References

1. Jabbour MN, Elder JB, Samuelson CG, Khashabi S, Hofman FM, Giannotta SL, Liu CY. Aberrant angiogenic characteristics of human brain arteriovenous

malformation endothelial cells. Neurosurgery 2009 Jan;64(1):139–46; discussion 146–8. doi: 10.1227/01.NEU.0000334417.56742.24. [PubMed: 19145162]

2. Al-Shahi R, Fang JS, Lewis SC, Warlow CP. *Prevalence of adults with brain arteriovenous* malformations: a community based study in Scotland using capture-recapture analysis. J Neurol Neurosurg Psychiatry 2002 Nov;73(5):547–51. doi: 10.1136/jnnp.73.5.547. [PubMed: 12397149]
3. Berman MF, Sciacca RR, Pile-Spellman J, Stapf C, Connolly ES Jr, Mohr JP, Young WL. The epidemiology of brain arteriovenous malformations. Neurosurgery 2000 Aug;47(2):389–96; discussion 397. doi: 10.1097/00006123-200008000-00023. [PubMed: 10942012]
4. Gilbo P, Zhang I, Knisely J. Stereotactic radiosurgery of the brain: a review of common indications. Chin Clin Oncol 2017 Sep;6(Suppl 2):S14. doi: 10.21037/cco.2017.06.07. [PubMed: 28917252]
5. Schneider BF, Eberhard DA, Steiner LE. Histopathology of arteriovenous malformations after gamma knife radiosurgery. J Neurosurg 1997 Sep;87(3):352–7. doi: 10.3171/jns.1997.87.3.0352. [PubMed: 9285598]
6. Park CK, Choi SK, Lee SH, Choi MK, Lim YJ. Clinical outcomes and radiosurgical considerations for pediatric arteriovenous malformation: influence of clinical features on obliteration rate. Childs Nerv Syst 2017 Dec;33(12):2137–2145. doi: 10.1007/s00381-017-3579-7. [PubMed: 28871374]
7. Chen JC, Mariscal L, Girvigian MR, Vanefsky MA, Glousman BN, Miller MJ, Feng L, Rahimian J. Hypofractionated stereotactic radiosurgery for treatment of cerebral arteriovenous malformations: outcome analysis with use of the modified arteriovenous malformation scoring system. J Clin Neurosci 2016 Jul;29:155–61. doi: 10.1016/j.jocn.2015.12.006. [PubMed: 26947340]
8. Starke RM, Kano H, Ding D, Lee JY, Mathieu D, Whitesell J, Pierce JT, Huang PP, Kondziolka D, Yen CP, Feliciano C, Rodgriguez-Mercado R, Almodovar L, Pieper DR, Grills IS, Silva D, Abbassy M, Missios S, Barnett GH, Lunsford LD, Sheehan JP. Stereotactic radiosurgery for cerebral arteriovenous malformations: evaluation of long-term outcomes in a multicenter cohort. J Neurosurg 2017 Jan;126(1):36–44. doi: 10.3171/2015.9.JNS151311. [PubMed: 26943847]
9. Missios S, Bekelis K, Al-Shyal G, Rasmussen PA, Barnett GH. Stereotactic radiosurgery of intracranial arteriovenous malformations and the use of the K index in determining treatment dose. Neurosurg Focus 2014 Sep;37(3):E15. doi: 10.3171/2014.7.FOCUS14157.
10. Yang SY, Paek SH, Kim DG, Chung HT. Quality of life after radiosurgery for cerebral arteriovenous malformation patients who present with seizure. Eur J Neurol 2012 Jul;19(7):984–91. doi: 10.1111/j.1468-1331.2012.03664.x. [PubMed: 22340506]
11. Huo X, Li Y, Wu Z, Jiang Y, Yang H, Zhao Y. Combined treatment of brain AVMs by Onyx embolization and gamma knife radiosurgery decreased hemorrhage risk despite low obliteration rate. Turk Neurosurg 2015;25(1):100–10. doi: 10.5137/1019-5149.JTN.10708-14.1. [PubMed: 25640553]
12. Sirin S, Kondziolka D, Niranjan A, Flickinger JC, Maitz AH, Lunsford LD. Prospective staged volume radiosurgery for large arteriovenous malformations: indications and outcomes in otherwise untreatable patients. Neurosurgery 2008 Feb;62 Suppl 2:744–54. doi: 10.1227/01.neu.0000316278.14748.87. [PubMed: 18596431]
13. Mirza-Aghazadeh J, Andrade-Souza YM, Zadeh G, Scora D, Tsao MN, Schwartz ML. Radiosurgical retreatment for brain arteriovenous malformation. Can J Neurol Sci 2006 May;33(2):189–94. doi: 10.1017/s0317167100004959. [PubMed: 16736728]
14. Alakbarzade V, Pereira AC. Cerebral catheter angiography and its complications. Pract Neurol 2018 Oct;18(5):393–398. doi: 10.1136/practneurol-2018-001986. [PubMed: 30021800]
15. Kano H, Kondziolka D, Flickinger JC, Yang HC, Flannery TJ, Awan NR, Niranjan A, Novotny J Jr, Lunsford LD. Stereotactic radiosurgery for arteriovenous malformations, Part 3: outcome predictors and risks after repeat radiosurgery. J Neurosurg 2012 Jan;116(1):21–32. doi: 10.3171/2011.9.JNS101741. [PubMed: 22077445]
16. Shaligram SS, Winkler E, Cooke D, Su H. Risk factors for hemorrhage of brain arteriovenous malformation. CNS Neurosci Ther 2019 Oct;25(10):1085–1095. doi: 10.1111/cns.13200. [PubMed: 31359618]
17. Stankovic Z, Allen BD, Garcia J, Jarvis KB, Markl M. 4D flow imaging with MRI. Cardiovasc Diagn Ther 2014 Apr;4(2):173–92. doi: 10.3978/j.issn.2223-3652.2014.01.02. [PubMed: 24834414]

18. Hsiao A, Alley MT, Massaband P, Herfkens RJ, Chan FP, Vasanawala SS. Improved cardiovascular flow quantification with time-resolved volumetric phase-contrast MRI. Pediatr Radiol 2011 Jun;41(6):711–20. doi: 10.1007/s00247-010-1932-z. [PubMed: 21221566]
19. Hsiao A, Yousaf U, Alley MT, Lustig M, Chan FP, Newman B, Vasanawala SS. Improved quantification and mapping of anomalous pulmonary venous flow with four-dimensional phase-contrast MRI and interactive streamline rendering. J Magn Reson Imaging 2015 Dec;42(6):1765–76. doi: 10.1002/jmri.24928. [PubMed: 25914149]
20. Meckel S, Leitner L, Bonati LH, Santini F, Schubert T, Stalder AF, Lyrer P, Markl M, Wetzel SG. Intracranial artery velocity measurement using 4D PC MRI at 3 T: comparison with transcranial ultrasound techniques and 2D PC MRI. Neuroradiology 2013 Mar;55(4):389–98. doi: 10.1007/s00234-012-1103-z. [PubMed: 23143179]
21. Cebral JR, Putman CM, Alley MT, Hope T, Bammer R, Calamante F. Hemodynamics in Normal Cerebral Arteries: Qualitative Comparison of 4D Phase-Contrast Magnetic Resonance and Image-Based Computational Fluid Dynamics. J Eng Math 2009 Aug 1;64(4):367–378. doi: 10.1007/s10665-009-9266-2. [PubMed: 19684874]
22. Bammer R, Hope TA, Aksoy M, Alley MT. Time-resolved 3D quantitative flow MRI of the major intracranial vessels: initial experience and comparative evaluation at 1.5T and 3.0T in combination with parallel imaging. Magn Reson Med 2007 Jan;57(1):127–40. doi: 10.1002/mrm.21109. [PubMed: 17195166]
23. Lorenz R, Bock J, Snyder J, Korvink JG, Jung BA, Markl M. Influence of eddy current, Maxwell and gradient field corrections on 3D flow visualization of 3D CINE PC-MRI data. Magn Reson Med 2014 Jul;72(1):33–40. doi: 10.1002/mrm.24885. [PubMed: 24006013]
24. Li CQ, Hsiao A, Hattangadi-Gluth J, Handwerker J, Farid N. Early Hemodynamic Response Assessment of Stereotactic Radiosurgery for a Cerebral Arteriovenous Malformation Using 4D Flow MRI. AJNR Am J Neuroradiol 2018 Apr;39(4):678–681. doi: 10.3174/ajnr.A5535. [PubMed: 29371257]
25. Imbesi SG, Knox K, Kerber CW. Reproducibility analysis of a new objective method for measuring arteriovenous malformation nidus size at angiography. AJNR Am J Neuroradiol 2002 Mar;23(3):412–5. [PubMed: 11901010]
26. Wen B, Tian S, Cheng J, Li Y, Zhang H, Xue K, Zhang Z, Fan Y, Wu B. Test-retest multisite reproducibility of neurovascular 4D flow MRI. J Magn Reson Imaging 2019 Jun;49(6):1543–1552. doi: 10.1002/jmri.26564. [PubMed: 30443945]
27. Stüer C, Ikeda T, Stoffel M, Luippold G, Sakowitz O, Schaller K, Meyer B. Norepinephrine and cerebral blood flow regulation in patients with arteriovenous malformations. Neurosurgery 2008 Jun;62(6):1254–60; discussion 1260–1. doi: 10.1227/01.neu.0000333296.41813.74. [PubMed: 18824991]
28. Diehl RR, Linden D, Lücke D, Berlit P. Phase relationship between cerebral blood flow velocity and blood pressure. A clinical test of autoregulation. Stroke 1995 Oct;26(10):1801–4. doi: 10.1161/01.str.26.10.1801. [PubMed: 7570728]
29. Schnell S, Wu C, Ansari SA. Four-dimensional MRI flow examinations in cerebral and extracerebral vessels - ready for clinical routine? Curr Opin Neurol 2016 Aug;29(4):419–28. doi: 10.1097/WCO.0000000000000341. [PubMed: 27262148]
30. Shakur SF, Amin-Hanjani S, Abouelleil M, Aletich VA, Charbel FT, Alaraj A. Changes in pulsatility and resistance indices of cerebral arteriovenous malformation feeder arteries after embolization and surgery. Neurol Res 2017 Jan;39(1):7–12. doi: 10.1080/01616412.2016.1258970. [PubMed: 27866455]
31. Naqvi J, Yap KH, Ahmad G, Ghosh J. Transcranial Doppler ultrasound: a review of the physical principles and major applications in critical care. Int J Vasc Med 2013;2013:629378. doi: 10.1155/2013/629378. [PubMed: 24455270]
32. Kuceyeski A, Shah S, Dyke JP, Bickel S, Abdelnour F, Schiff ND, Voss HU, Raj A. The application of a mathematical model linking structural and functional connectomes in severe brain injury. Neuroimage Clin 2016 Apr 14;11:635–647. doi: 10.1016/j.nicl.2016.04.006. [PubMed: 27200264]

33. Harris NG, Verley DR, Gutman BA, Thompson PM, Yeh HJ, Brown JA. Disconnection and hyper-connectivity underlie reorganization after TBI: A rodent functional connectomic analysis. Exp Neurol 2016 Mar;277:124–138. doi: 10.1016/j.expneurol.2015.12.020. [PubMed: 26730520]

34. Kasahara M, Menon DK, Salmond CH, Outtrim JG, Taylor Tavares JV, Carpenter TA, Pickard JD, Sahakian BJ, Stamatakis EA. Altered functional connectivity in the motor network after traumatic brain injury. Neurology 2010 Jul 13;75(2):168–76. doi: 10.1212/WNL.0b013e3181e7ca58. [PubMed: 20625170]

35. Aristova M, Vali A, Ansari SA, Shaibani A, Alden TD, Hurley MC, Jahromi BS, Potts MB, Markl M, Schnell S. Standardized Evaluation of Cerebral Arteriovenous Malformations Using Flow Distribution Network Graphs and Dual-venc 4D Flow MRI. J Magn Reson Imaging 2019 Dec;50(6):1718–1730. doi: 10.1002/jmri.26784. [PubMed: 31070849]

36. Homan RW, Devous MD Sr, Stokely EM, Bonte FJ. Quantification of intracerebral steal in patients with arteriovenous malformation. Arch Neurol 1986 Aug;43(8):779–85. doi: 10.1001/archneur.1986.00520080027015. [PubMed: 3488052]

37. Mast H, Mohr JP, Osipov A, Pile-Spellman J, Marshall RS, Lazar RM, Stein BM, Young WL. 'Steal' is an unestablished mechanism for the clinical presentation of cerebral arteriovenous malformations. Stroke 1995 Jul;26(7):1215–20. doi: 10.1161/01.str.26.7.1215. [PubMed: 7604417]

38. Dunås T, Holmgren M, Wåhlin A, Malm J, Eklund A. Accuracy of blood flow assessment in cerebral arteries with 4D flow MRI: Evaluation with three segmentation methods. J Magn Reson Imaging 2019 Aug;50(2):511–518. doi: 10.1002/jmri.26641. [PubMed: 30637846]

39. Oermann EK, Rubinsteyn A, Ding D, Mascitelli J, Starke RM, Bederson JB, Kano H, Lunsford LD, Sheehan JP, Hammerbacher J, Kondziolka D. Using a Machine Learning Approach to Predict Outcomes after Radiosurgery for Cerebral Arteriovenous Malformations. Sci Rep 2016 Feb 9;6:21161. doi: 10.1038/srep21161. [PubMed: 26856372]

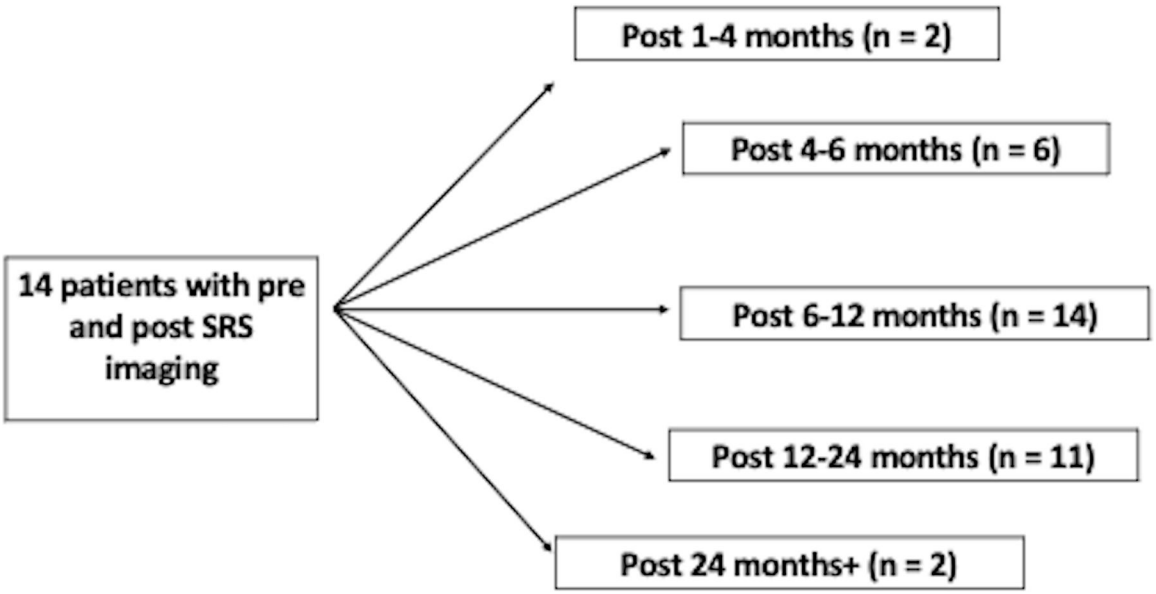

Figure 1.

Flowchart of patients included in this study and time points of respective 4D Flow measurements. 14 patients had pre and post SRS imaging, and were included in this study. The timepoints of post-SRS imaging are as listed in the figure.

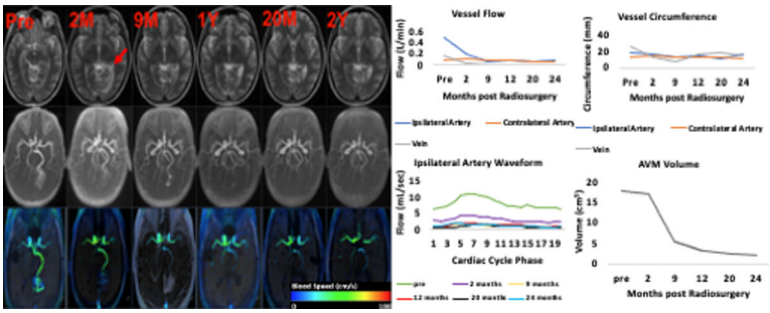

Figure 2.

This is a 33 year old female with Spetzler-Martin grade 3 left posterior temporal-occipital AVM treated with a single-stage of SRS (1600 cGy). Of note, there is post-radiation edema visualized in the peri-nidal region (arrow) on T_2W imaging at the 2 month time point (2A) which subsequently resolves. While T_2W imaging (3A) and MRA (2B) demonstrate gradual decrease of the nidus from before SRS to 2 years after SRS, 4D Flow (2C) demonstrates early attenuation in blood flow within the feeding artery and draining vein. There is a 61.2% reduction in feeding artery blood flow and 76.5% reduction in draining vein blood flow by 2 months, and normalization of feeding artery blood flow by 2 years (2D). In comparison, there is only 2.3% reduction in feeding artery circumference with a more substantial reduction in draining vein circumference (50.6%) by 2 months (2E). There is an increase in pulsatility of the ipsilateral artery after 20 moths post treatment (2F). There is initially a gradual decrease in AVM volume followed by a significant decrease at 9 months (2G).

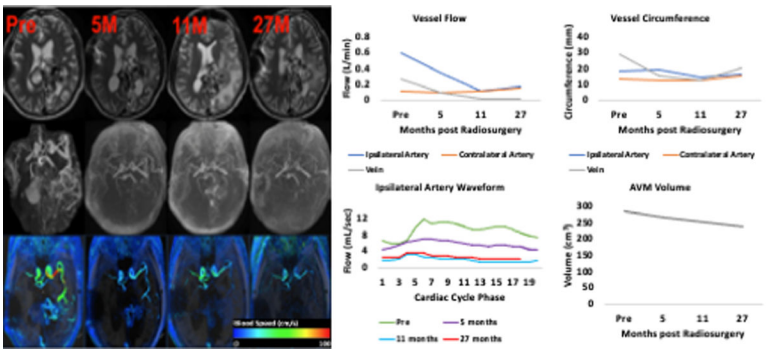

Figure 3.

This is a 44 year old male with Spetzler-Martin grade 5 periventricular/pericallosal AVM treated with embolization followed by a single-stage of SRS (2000 cGy). T_2W imaging (3A) and MRA (3B) demonstrate subtle and gradual decrease in nidus volume while 4D Flow (3C) demonstrates attenuation in blood flow within the feeding artery and draining vein. There is a 43.3% reduction in feeding artery blood flow and 63.0% reduction in draining vein blood flow by 5 months, and normalization of feeding artery blood flow by 27 months (3D). In comparison, there is only 5.8% increase in feeding artery circumference with a more substantial reduction in draining vein circumference (46.6%) by 5 months (3E). There is no clear trend in pulsatility of the ipsilateral artery after treatment (3F). There is a subtle and gradual decrease in AVM volume with 83.9% of the AVM volume still present at 27 months post treatment(3G).

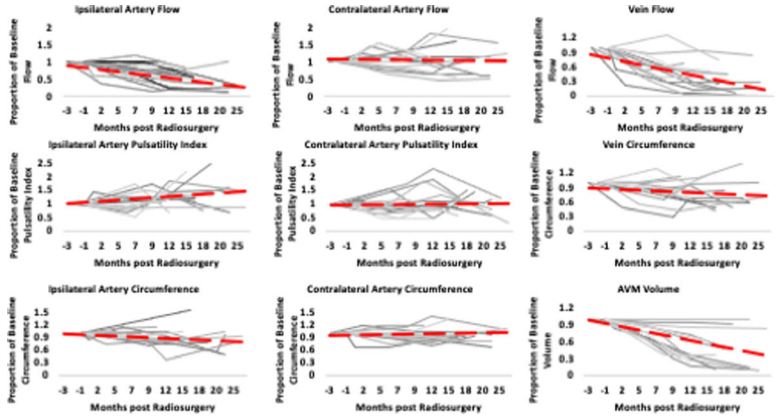

Figure 4.

Aggregate line graphs with linear trend line of ipsilateral and contralateral artery flow, circumference, and pulsatility index, and venous flow, circumference, and AVM volume in relation to time since radiosurgery. Three patients had 4D flow measurements in between SRS stages. There is a general trend in decrease in ipsilateral artery flow, vein flow, vein circumference, and AVM volume over time. There is an increase in ipsilateral artery pulsatility over time. There is not a consistent trend for change in circumference of ipsilateral or contralateral artery, or contralateral artery pulsatility over time. Patients with higher grade AVMs demonstrated minimal change in AVM volume up to 27 months post-SRS.

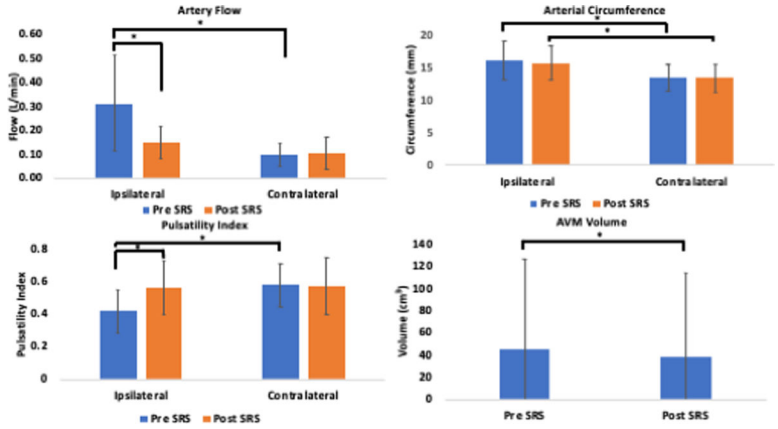

Figure 5.

Bar graph of total changes in ipsilateral and contralateral artery flow, circumference, pulsatility index, and AVM volume before and after SRS. Median follow-up for post-SRS imaging was 12 months (range: 11 – 16 months). Ipsilateral artery flow was significantly greater than contralateral artery flow pre-SRS and decreased significantly post-SRS. Ipsilateral artery circumference was greater than contralateral artery circumference before and after SRS. Ipsilateral artery pulsatility was lower than contralateral artery pulsatility prior to SRS and increased significantly after SRS. Volume significantly decreased after SRS.

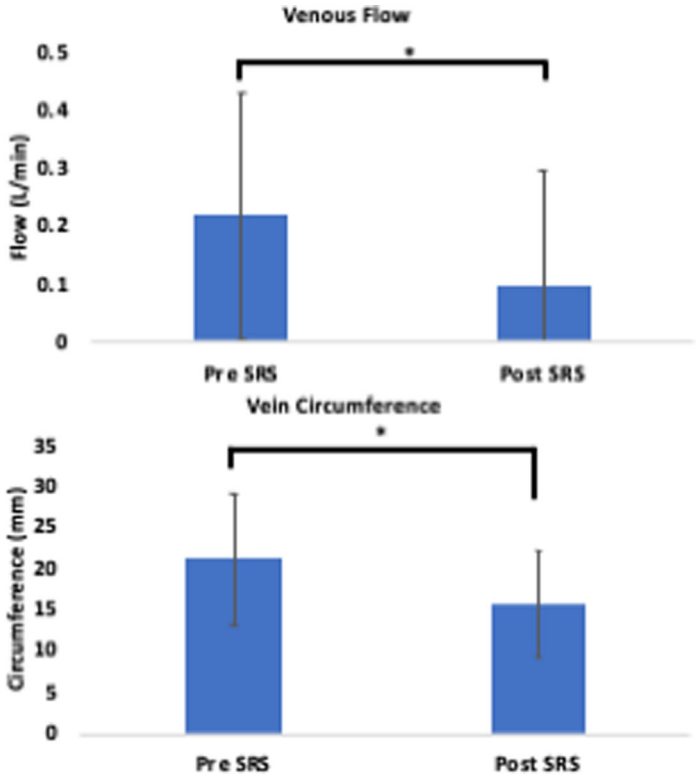

Figure 6.

Bar graph of average changes in venous flow and circumference before and after SRS. Median follow-up for post-SRS imaging was 12 months (range: 11 – 16 months). There is a significant decrease in venous flow and circumference after SRS.

Table I.

Demographics of patients included in this study. There were 6 females and 8 males included. Distribution of SM grades was as follows - SM 2 (3), SM 3 (7), SM 4 (2), SM 5 (2). Patient 13, 18, and 21 had 4D flow MRI imaging in between SRS treatments.

Patient Number	Age at Start of Treatment	Sex	AVM Location	AVM SM Grade	Treatment	Dose of Radiation (cGy)
3	50	Female	right temporal	2	embolization followed by single-stage SRS	2000
4	30	Male	right temporal/occipital	4	single-stage SRS	2000
8	33	Female	left posterior temporal/ occipital	3	single-stage SRS	1600
13*	36	Female	pericallosal	5	embolization followed by 2-stage SRS	2000 (x2)
17	34	Female	quadrigeminal plate cistern	3	single-stage SRS	2000
18*	38	Male	right temporal/occipital	3	coiling of ruptured AVM followed by 2-stage SRS	2000 1900
19	21	Male	right medial parieto-occipital sulcus	3	embolization of ruptured AVM followed by single-stage SRS	2000
20	60	Female	posteriomedial left temporal lobe (posterior to temporal horn of lateral ventricle)	2	single-stage SRS	2100
21*	54	Male	right frontal lobe	4	surgical evacuation of ruptured AVM followed by embolization and 3-stage SRS	1800 (x3)
22	44	Male	left fronto-periventricular/ pericallosal	5	embolization followed by single-stage SRS	2000
23	76	Male	torcula	3	single-stage SRS	2100
26	52	Male	left parietal lobe	3	coiling of AVM aneurysm followed by single-stage SRS	2000
27	64	Female	left parietal/temporal lobe	2	single-stage SRS	2200
28	28	Male	left occipital	3	embolization of ruptured AVM followed by single-stage SRS	2200